

Experimental Study on Utilization of Coal Ash to R/C Members

Kenji Kabayama and Hideo Araki

Graduate School of Engineering, Hiroshima University, Higashi-hiroshima, Japan 739-8527

Shunsuke Sugano

Graduate School of Engineering, Hiroshima University, Higashi-hiroshima, Japan 739-8527

(Received 23 June 2003)

Coal ash, produced by coal-fired power plants, is one of industrial by-products against to the environmental conservation. Utilization of the coal ash is an urgent and important objective for the ecological and resources problem. Static loading tests were carried out to investigate shear characteristics of short R/C columns containing high volume coal ash, which included both fly ash and cinder ash. Lateral strength of the columns was able to estimated by the proposed formula for R/C members used normal concrete. The columns had better ductility than the column of the similar shape without coal ash. From these results, it is anticipated that there is strong possibility of using concrete containing high volume coal ash for R/C building structural members.

Keywords: Coal ash, environmental conservation, concrete, short R/C column, building structural member.

1. Introduction

The amount of industrial by-products, such as coal ash produced by coal-fired power plants, continues to increase with the demand for more electricity. It is said that total quantities of coal ash produced in Japan will be more than 10,000,000 tons in a couple of years [1]. Utilization of coal ash is a very urgent objective. At present, about 60% of coal ash is utilized as cement material or admixture. The remainder is thrown away in landfill although they include good properties, corresponding to Japanese Industrial Standard (JIS) for fly ash. Utilization of the large quantity of coal ash to concrete manufacturing is not only effective in increasing the use percentage, but also able to reduce the consumption of other natural material, such as aggregates that has been nearly depleted. In order to consume a large quantity of coal ash, the characteristics of concrete containing high volume coal ash have been investigated recently through the small size cylinder tests [2, 3]. It has been clarified that mechanical properties and durability of hardened concrete containing high volume coal ash were not so different from concrete without coal ash. The mechanical characteristics of reinforced concrete, R/C, members containing high volume coal ash should be investigated in order to utilize to building structural members. Several static loading tests have been carried out by authors to investigate the seismic performance of R/C members

containing high volume coal ash, which included both fly ash and cinder ash [4, 5]. The specimens were beams which were designed as the flexural failure type, and columns which were designed as the shear-flexural failure type. Those test results revealed that the specimens had enough seismic performance regardless of coal ash content. Static loading tests of short R/C columns, which were carried out to investigate shear characteristics of R/C members containing high volume coal ash, were reported in this paper. Test parameters considered in this study was a mix property for concrete containing coal ash.

2. Scope of Experimental Investigation

2.1. Design of Mix Properties and Used Materials

Coal ash used in this study was produced at a coal-fired power plant located in Yamaguchi Prefecture, Japan. The physical properties and grain size distributions of the coal ash, containing both fly ash and cinder ash, are shown in Table 1 and Fig. 1. The physical properties are corresponded to the II class of JIS for fly ash.

Considered parameter in this study was a mix property for concrete containing coal ash. Four type of mix properties, normal concrete [NC], concrete containing coal ash as a partial replacement of fine aggregate [CA20 and CA40], and high fluidity concrete containing coal ash as a partial replacement of cement [HF] were assigned

Table 1

Physical properties of used coal ash.

Moisture (%)	Loss on ignition (%)	Density (g/cm ³)	Blaine (cm ² /g)
Less than 0.1	2.30	2.16	2,840

in four test columns. Summaries of mix properties for each concrete are shown in Table 2. The properties of CA20, CA40 and HF were selected as the most practical case, based on preliminary mixing tests in the laboratory. The volume of coal ash was 20% and 40% of total volume of fine aggregate in CA20 and CA40, respectively. The weight of coal ash was equal to the weight of cement in HF. Compressive strength at 28 day was 36N/mm² (MPa), and the air content was 4.5%. Those were common conditions for design of mixtures. In design for workability, slump was 18cm for NC, CA20 and CA40, slump flow was 65cm for HF. The maximum size of used coarse aggregate, that was crashed stone, was 20mm. The fine aggregate was the mixture of pit sand and fine sand.

Evaluation of compressive strength of concrete with curing age is shown in Fig. 2. These results were obtained by compressive tests using thirty 10×20cm cylinders. Those cylinders, which were placed in the air after casting, were demolded at the age of 3 days. Those demolded cylinders were exposed to the air in the same laboratory as test columns. When the compressive strength of concrete reached to the design strength 36N/mm², loading tests of columns were performed. The measured mechanical properties of concrete at the test age are shown in Table 3.

2.2. General Test Procedure

Test columns had large stubs on their top and bottom as detailed in Fig. 3 (a). The test column, whose section was 200×200mm and whose height was 400mm, was designed as approximately 1/4-scaled model of the prototype column. Shear span ratio (M/QD) was 1.0. Reinforcing bars, 8-D10, were used as the longitudinal bars, and the hoop reinforcement was 2-4φ @50mm. They were designed as the shear failure type according to the R/C standard of Japan [6]. The test setup is shown in Fig. 3 (b). Cyclic lateral loadings were carried out under the constant axial load, which was 10% of axial load capacity of the column ($F_C bD$). The axial load, N , was applied

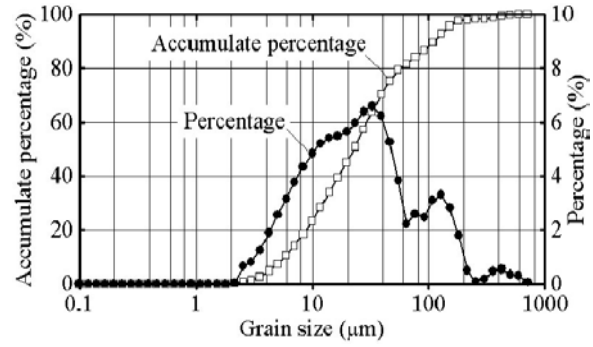


Figure 1. Grain size distributions of used coal ash

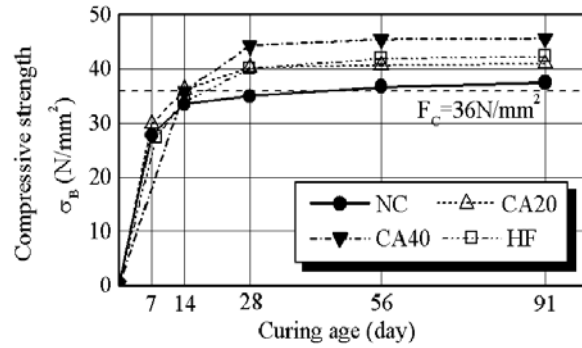


Figure 2. Compressive strength of concrete

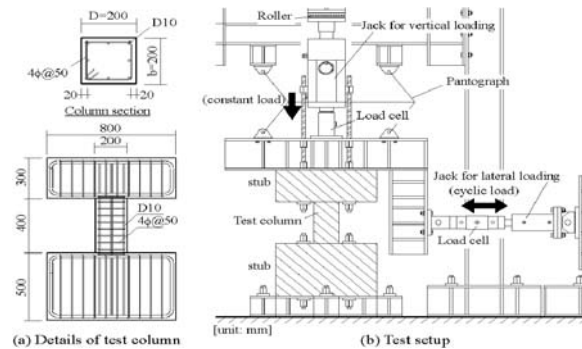


Figure 3. Details of test column and test setup

Table 2
Summaries of mix properties for concrete

Test column	W/(C+Ca) ratio (%)	Unit (kg/m ³)					
		Water	Bulk material		Fine aggregate		Coarse aggregate
			Cement	Coal ash	Sand	Coal ash	
NC	43	187	435	0	748	0	921
CA20	37	180	360	0	591	121	1,022
CA40	31	180	330	0	489	247	1,000
HF	31	175	285	285	698	0	785

W; Water, C; Cement, Ca; Coal ash

at the top of the test column. The cyclic lateral loadings were controlled by monitoring drift angle, R , which was shown in Fig. 4. The amplitude of the drift angle was increased carefully from very small level as shown in the same figure.

3. Test Results and Discussions

3.1. Crack Patterns and Hysteresis Loops

Crack patterns at the failure stage of each test are shown in Fig. 5. All specimens had almost similar crack propagations and damaged area during the loadings. There was no influence of coal ash content on the crack patterns. The first flexural cracks occurred at the top and bottom ends up to $R=1/800$ rad. in all test columns. Diagonal shear cracks were observed after $R=1/400$ rad. in each test, and both lateral strength and axial load rapidly decreased with shear failure.

Fig. 6 shows lateral load-displacement hysteresis loops of each test column. The shear cracking point and the shear failure point were marked in each hysteresis loops. Shapes of the loops were very slender spindle types in each test due to shear behavior. The shear failure occurred just after $R=1/400$ rad. in NC, while they occurred after $R=1/200$ rad. in CA20, CA40 and HF.

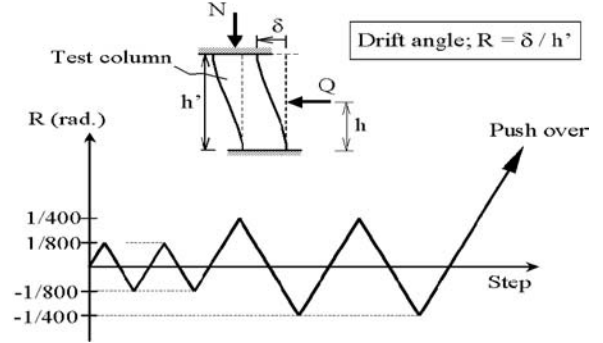


Figure 4. Drift angle and Lateral loading history

3.2. Maximum Lateral Strength

Comparisons between the measured maximum lateral strength and calculated ultimate strength of each test column are shown in Table 4. Calculated results for the ultimate flexural strength, Q_M , and the ultimate shear strength, Q_S , were obtained by Eq.1 and Eq.2, respectively [6]. There are good agreements between test results and the calculated strength in each test column, although the used equations in this paper have been provided by AIJ for R/C members used normal concrete. It is confirmed that those equations are applicable to estimate the ultimate flexural strength or the ultimate shear strength for R/C members containing high volume coal ash.

Table 3
Measured concrete properties at the test age

Test column	Test age (day)	σ_B (N/mm ²)	σ_t (N/mm ²)	E_C (N/mm ²)
NC	34	36.0	2.96	2.65×10^4
CA20	15	36.8	2.85	3.27×10^4
CA40	20	41.8	3.08	2.99×10^4
HF	20	38.4	3.05	2.76×10^4

σ_B ; compressive strength, σ_t ; tensile strength, E_C ; Young's modulus

Table 4

Measured and calculated maximum strength

Test column	Measured Q_E (kN)	Calculated		Meas./Cal.	
		Q_M (kN)	Q_S (kN)	Q_E/Q_M	Q_E/Q_S
NC	136	147	121	0.93	1.12
CA20	136	149	122	0.91	1.11
CA40	143	158	131	0.91	1.09
HF	147	152	125	0.97	1.18

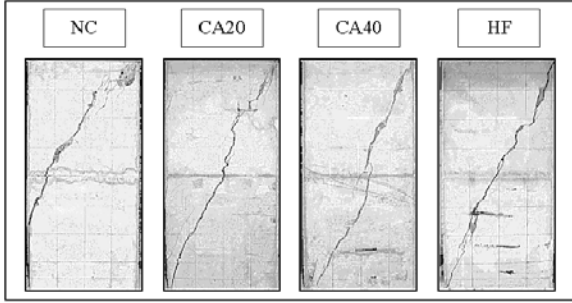
 Q_M ; Ultimate flexural strength, Q_S ; Ultimate shear strength


Figure 5. Crack patterns at the failure stage

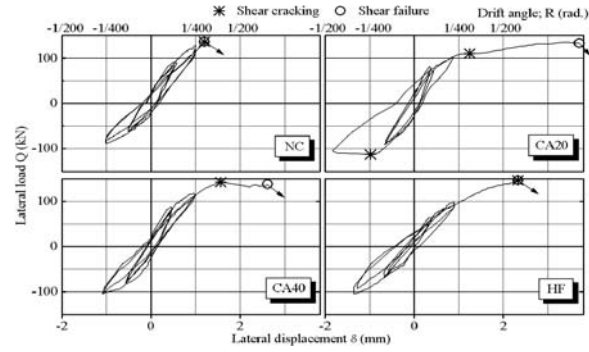


Figure 6. Lateral load-displacement hysteresis loops

$$Q_M = M_U/h \quad (1)$$

$$Q_S = (\tau_U + 0.1\sigma_0)bj \quad (2)$$

$$M_U = 0.8a_t\sigma_Y D + 0.5ND[1 - N/(bD\sigma_B)] \quad (3)$$

$$\tau_U = \frac{0.092k_U k_P (180 + \sigma_B)}{(M/Qd) + 0.12} + 2.7\sqrt{p_W \sigma_{WY}} \quad (4)$$

$$\sigma_0 = N/bD \quad (5)$$

a_t ; area of tensile reinforcing bar, b , D , j ; width, depth and lever arm of section, h ; height of lateral loading point, k_U , k_P ; coefficients related to section, M/Qd ; shear span ratio, N ; axial load, p_W ; ratio of hoop, σ_B ; compressive strength of concrete, σ_{WY} ; yield strength of hoop, σ_Y ; yield strength of longitudinal reinforcing bar

3.3. Shear Deformation and Ductility

The relationships of angular deformation and drift angle of each test column are shown in Fig. 7. The angular deformation was calculated at each peak point of lateral hysteresis loops based on diagonal displacements measured by transducers set to the test column as shown in the figure. The relationships are almost linear and similar in

each test before the shear cracking point, regardless of coal ash content. There was no harmful influence of coal ash content to shear deformation.

Table 5 shows lateral displacement and drift angle at the shear cracking point and the shear failure point of each test. Values of CA20, CA40 and HF, i.e. coal ash content type, are greater than NC at the shear failure point, while values at the shear cracking point are scattering. Displacements at the shear cracking point and the shear failure point of each test are normalized by the displacement at the shear failure point of NC in Fig. 8, while shear stress is normalized by tensile strength of concrete. The figure shows that ductility of CA20, CA40 and HF exceed the case of NC more than approximately 2 times. It is indicated that coal ash content improved the ductility of shear members.

4. Concluding Remarks

Seismic loading tests of scaled R/C members containing high volume coal ash were performed.

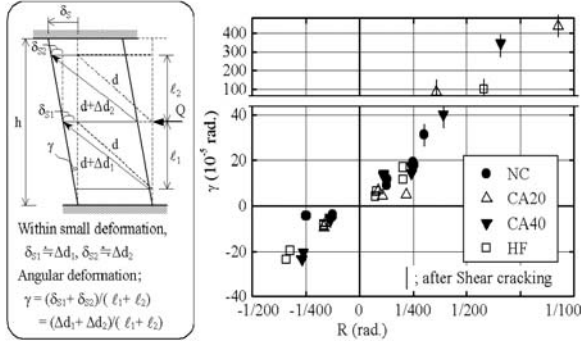


Figure 7. Angular deformation and drift angle

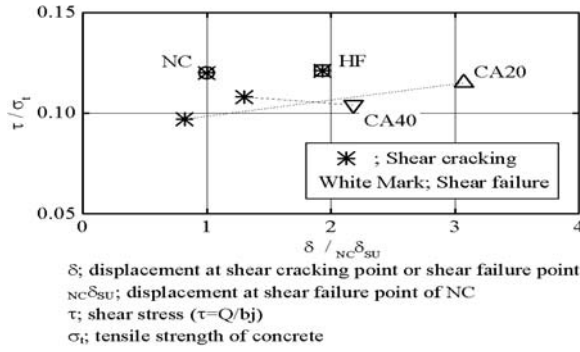


Figure 8. Ductility and shear stress

Specimens were short R/C columns designed as the shear failure type. Coal ash content in concrete was the parameter. Test results indicated following remarks.

1. No harmful influence of coal ash content was observed in each test.
2. Equations of the ultimate flexural strength and the ultimate shear strength for R/C member used normal concrete were applicable to members containing high volume coal ash.
3. There was possibility that coal ash content improved the ductility of shear members.

It is anticipated that there is strong possibility of utilizing concrete containing high volume coal ash for building structural members.

Table 5

Comparisons of ductility. Disp: Displacement

Test column	Shear cracking		Shear failure	
	Disp δ_{SC} (mm)	Drift angle R_{SC} (rad.)	Disp δ_{SU} (mm)	Drift angle R_{SU} (rad.)
NC	1.20	1/332	1.20	1/332
CA20	0.99	1/404	3.70	1/108
CA40	1.56	1/256	2.63	1/152
HF	2.33	1/172	2.33	1/172

5. Acknowledgements

This research work was performed as a joint research project between Hiroshima University and Chugoku Electric Power Co., Inc. The part of this research has been supported by Japan Ministry of Education, Culture, Sports, Science and Technology under Grant-in-aid No.11650587. Authors wish to thank every staffs and graduate students of Structural and Earthquake Engineering Lab., Hiroshima University.

References

- [1] JCAA, Coal Ash Hand-book 2nd Edition, (Tokyo, 1995).
- [2] M. V. Malhotra, Investigations of High-Volume Fly Ash Concrete Systems, EPRI TR-10315 Project 3176-66 Final Report (1993).
- [3] T. Tanigawa, et al. Characteristics of Concrete Containing a Large Amount of Coal-Ash, Proc. of Japan Concrete Institute, **17**, 331 (Tokyo, 1995)
- [4] H. Araki, K. Kabayama and T. Fukushima, Experimental Study on Seismic Performance of RC Members Containing High Volume Coal Ash. Proc. of 2001 Second International Conference on Engineering Materials, **1**, 465, San Jose (2001).
- [5] H. Araki, K. Kabayama, and T. Fukushima, Seismic Performance of RC Columns Containing High Volume Coal Ash. Proc. of the Third International Conference on Concrete under Severe Conditions, **1**, 652, Vancouver (2001).
- [6] AIJ, Standard for Structural Calculation of Reinforced Concrete Structures (Tokyo,1999).